

Supplementary Information

Stable dinitrile end-capped closed-shell non-quinodimethane as donor, acceptor and additive of organic solar cells

Weixuan Liang,[†] Peng Liu,[†] Yiheng Zhang, Weiya Zhu, Xinyang Tao, Zhicai He* & Yuan Li*

Institute of Polymer Optoelectronic Materials and Devices, State Key Laboratory of Luminescent Materials and Devices, South China University of Technology, Guangzhou, 510640, P.R. China,

[†]These authors contributed equally to this work.

E-mail: celiy@scut.edu.cn, zhicaihe@scut.edu.cn

Contents

1	Materials and instruments	3
2	Device fabrication and characterizations	3
3	Synthesis process of CN-Br and YF-CN	4
4	¹ H-NMR and MALDI-TOF mass spectra.....	6
	Fig. S1. ¹ H-NMR spectrum of CN-Br in CDCl ₃	6
	Fig. S2. ¹ H-NMR spectrum of CN-Br in the aromatic region in CDCl ₃	6
	Fig. S3. ¹ H-NMR spectrum of YF-CN in CDCl ₃	7
	Fig. S4. ¹ H-NMR spectrum of YF-CN in the aromatic region in CDCl ₃	7
	Fig. S5. The high resolution MALDI-TOF mass spectrum of YF-CN.	8
5	Additional Figures	8
	Fig. S6. Normalized absorption spectra of YF-CN in CHCl ₃ solution and thin-film spin-coated with YF-CN in toluene solution.....	8
	Fig. S7. Cyclic voltammetry of (a) YF-CN and (b) Y6.....	9
	Fig. S8. UPS spectrum of the neat YF-CN film.	9
	Fig. S9. Photoluminescence spectra of pure donor, acceptor and their blend films. (a) excited at 500 nm, (b) excited at 650 nm.	10
	Fig. S10. (a) J-V curves and (b) EQE curves of PCE10:YF-CN:Y6-based ternary devices with different blending ratios.	11
	Fig. S11. Current density-voltage curves for the (a) electron and (b) hole mobility measurements of the blend films.....	12
	Fig. S12. Fluorescence microscopy images in different sizes for (a, b) fresh PCE10:Y6, (e, f) aged PCE10:Y6, (c, d) fresh PCE10:YF-CN:Y6 and (g, h) aged PCE10:YF-CN:Y6.....	13
6	Additional Tables.....	14
	Table S1. The photovoltaic parameters of the binary and ternary OSCs with different YF-CN ratio.	14
	Table S2. The electron mobilities (μ_e) and hole mobilities (μ_h) of the binary and ternary devices.	14
	Table S3. The photovoltaic parameters of the binary and ternary OSCs with the fresh and aged for 360 hours at room temperature.	14

1 Materials and instruments

All the chemicals and solvents were commercially available and used without further purification. The tin reagent BTP used in the synthesis process was commercially purchased from eFlexPV Limited. PCE10 was purchased from Sigma-Aldrich and Y6 was purchased from Organtec Ltd. The nuclear magnetic resonance (NMR) spectra of the materials were measured on a Bruker AV 400 MHz spectrometer in CDCl_3 at room temperature. UV-vis absorption spectra were conducted on a UV-3600 spectrophotometer. Cyclic voltammetry of targeted films were carried out on CHI660e electrochemical workstation in electrolyte solution of 0.1 M tetrabutylammonium hexafluorophosphate (Bu_4NPF_6) by using $\text{Hg}/\text{Hg}_2\text{Cl}_2$ reference electrode and a platinum counter electrode, respectively. The potential of $\text{Hg}/\text{Hg}_2\text{Cl}_2$ reference electrode was internally calibrated as 0.31 eV by using the ferrocene/ferrocenium redox couple (Fc/Fc^+), which has a known reduction potential of -4.80 eV.

AFM measurement: The AFM height and phase images were recorded on a Nanoscope AFM microscope (Bruker), where the tapping mode was used. The sample were fabricated in accordance with the conditions of the best devices.

SCLC measurements: Single carrier devices were fabricated, and the mobility of holes and electrons were measured by using the space charge limited current measurements. The structure of hole-only device was ITO/PEDOT:PSS/active layer/ MoO_3 /Ag and ITO/ ZnO /active layer/PDINO/Ag for electron-only device. Analyzing in the space charge limited regime, the charge mobility is fitting by Mott-Gurney equation:

$$J = 9\epsilon_r\epsilon_0\mu V^2/8d^3$$

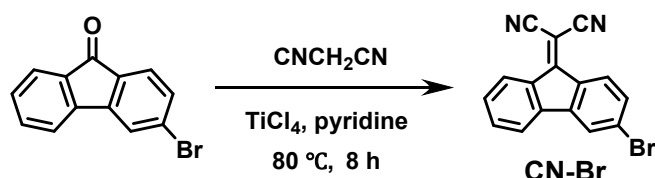
where ϵ_0 is the permittivity of vacuum, ϵ_r is the relative dielectric constant, d is the thickness of the active layer, V is the effective voltage, and μ is the mobility.

2 Device fabrication and characterizations

The organic solar cells were fabricated with a structure of ITO/PEDOT:PSS/active layer/PDINO/Ag. After 3 minutes of plasma treatment, the precleaned ITO substrates were coated with 40 nm PEDOT:PSS, followed by 15 minutes annealing at 150°C . PCE10:YF-CN (1:1.5, w/w) and YF-CN:Y6 (1:1, w/w) were all dissolved in chlorobenzene at the concentration of 20 mg/mL overnight at 60°C . PCE10:Y6 (1:1.5, w/w) and PCE10:YF-CN:Y6 (0.8:0.2:1.5, w/w) were prepared in chloroform at the concentration of 16 mg/mL and then stirred at 50°C overnight. All the solution of active layer were spin-coated onto PEDOT:PSS layer to obtain

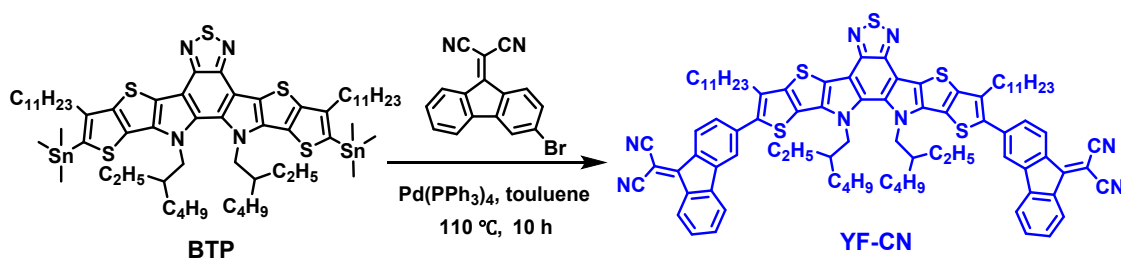
films thickness of about 120 nm. The methanol solution PDINO at a concentration of 1 mg/mL was spun on top of the active layer at 3000 rpm for 40s. Finally, 100 nm Ag was deposited in vacuum with a shadow mask at a pressure of about 3.0×10^{-4} Pa. The area of the devices was 0.057 cm^2 .

3 Synthesis process of CN-Br and YF-CN



Synthesis of 2-(3-bromo-9H-fluoren-9-ylidene)malononitrile (CN-Br)

3-Bromo-9H-fluoren-9-one (3.00 g, 0.012 mmol) and malononitrile (4.58 g, 0.07 mmol) in 30 mL of chloroform and 5 mL anhydrous pyridine under argon atmosphere, and then heated to 80°C and soaked for 0.5 h. 14 mL of chloroform solution of titanium tetrachloride (1 mol/L) was added to the reaction solution and the mixture was stirred at 80°C for 8 h. After the reaction was completed, the mixture was cooled to room temperature and extracted three times with dichloromethane. The crude product was purified by column chromatography (silica gel, petroleum ether/dichloromethane, v/v, 3:1) to afford CN-Br as a yellow-brown solid compound (3.28 g, 92.4 %). $^1\text{H-NMR}$ (CDCl_3 , 400 MHz) δ 8.40 (d, $J = 7.9$ Hz, 1H), 8.23 (d, $J = 8.4$ Hz, 1H), 7.71 (d, $J = 1.8$ Hz, 1H), 7.57-7.50 (m, 2H), 7.47 (d, $J = 8.4$, 1H), 7.40-7.35 (m, 1H).



Synthesis of YF-CN

Compound CN-Br synthesized in the previous step (45 mg, 0.148 mmol), the tin reagent BTP (80 mg, 0.062 mmol), $\text{Pd}(\text{PPh}_3)_4$ (16 mg, 0.014 mmol) and toluene (15 mL) were mixed and stirred under nitrogen atmosphere, and then heated to 110°C and soaked for 10 h. After the reaction was completed, the mixture was cooled to room temperature and extracted three times with dichloromethane. The crude product was purified by column chromatography (silica gel,

petroleum ether/dichloromethane, v/v, 2:1) to afford YF-CN as a navy blue solid compound (75 mg, 85.8%). ¹H-NMR (CDCl₃, 400 MHz) 8.50 (d, *J* = 8.2 Hz, 2H), 8.44 (d, *J* = 7.8 Hz, 2H), 7.75 (s, *J* = 1.7 Hz, 2H), 7.70-7.45 (m, 6H), 7.43-7.37 (m, 2H), 4.65 (m, 4H), 3.01 (m, 4H), 2.12-2.05 (m, 2H), 1.99-1.90 (m, 4H), 1.49 (m, 8H), 1.42-1.16 (m, 30H), 1.10 (m, 4H), 0.96 (m, 10H), 0.87 (m, 6H), 0.66 (m, 12H). HR-MS (MALDI-TOF) *m/z* calcd. for (C₈₈H₉₄N₈S₅): 1423.62. Found: 1423.2657.

4 $^1\text{H-NMR}$ and MALDI-TOF mass spectra

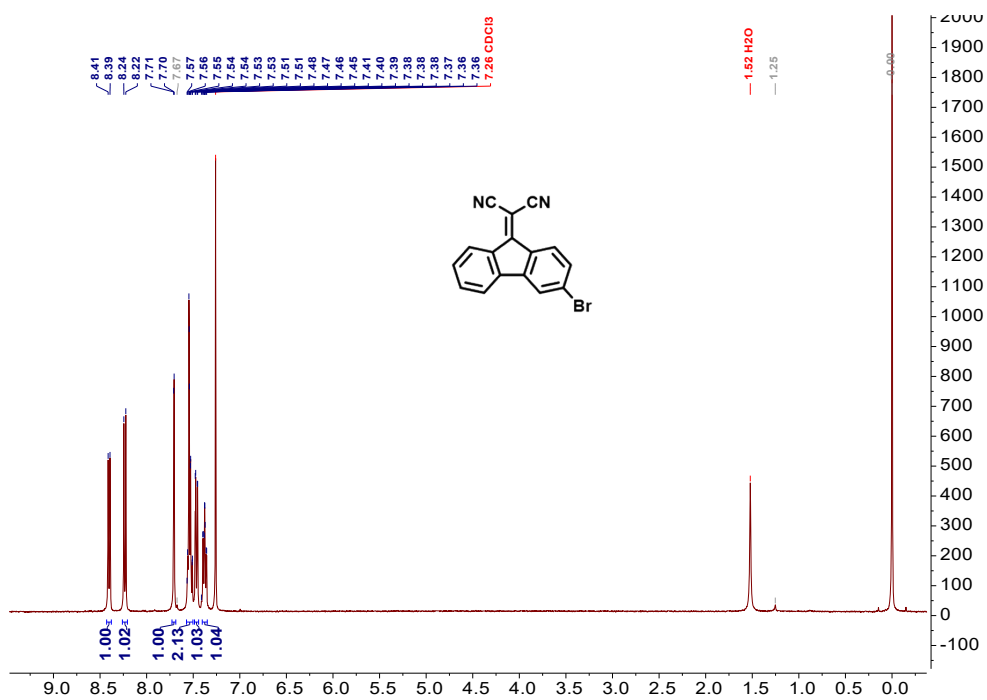


Fig. S1. $^1\text{H-NMR}$ spectrum of CN-Br in CDCl_3 .

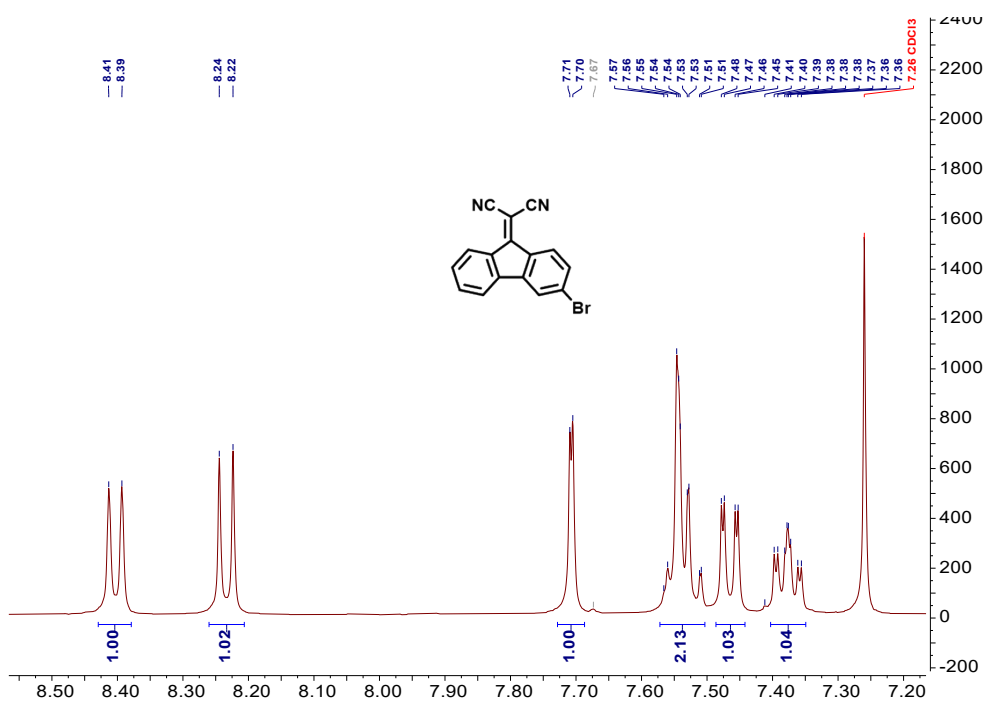


Fig. S2. $^1\text{H-NMR}$ spectrum of CN-Br in the aromatic region in CDCl_3 .

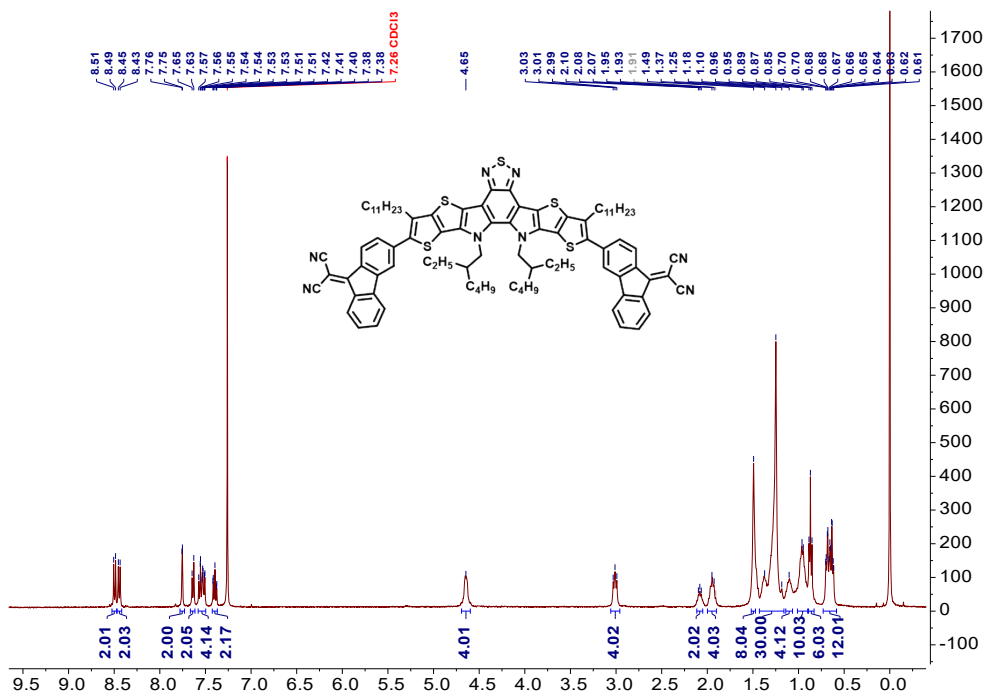


Fig. S3. ¹H-NMR spectrum of YF-CN in CDCl₃.

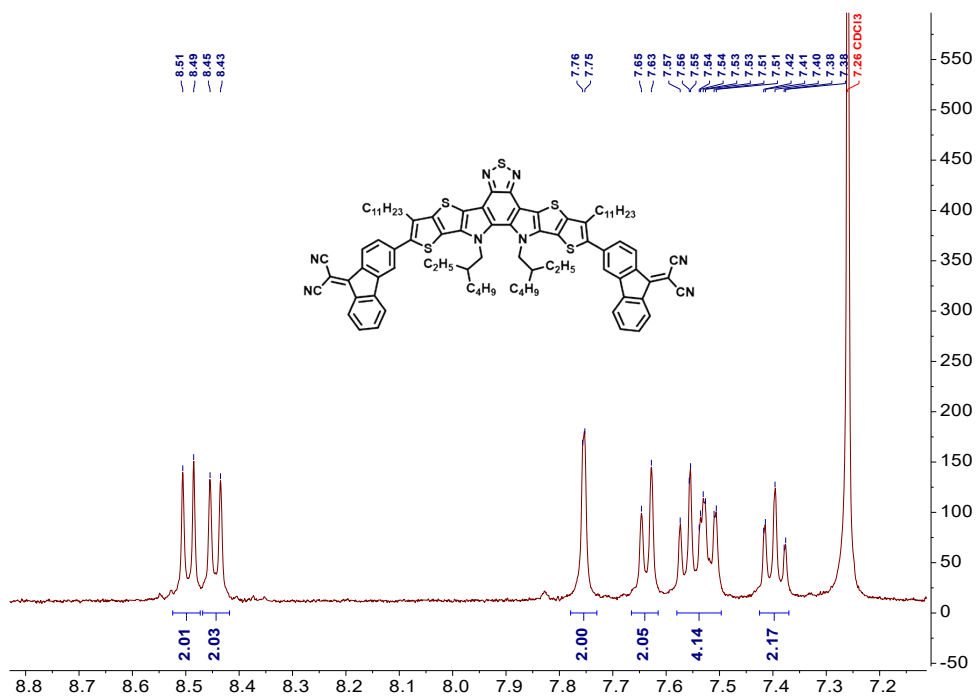


Fig. S4. ¹H-NMR spectrum of YF-CN in the aromatic region in CDCl₃.

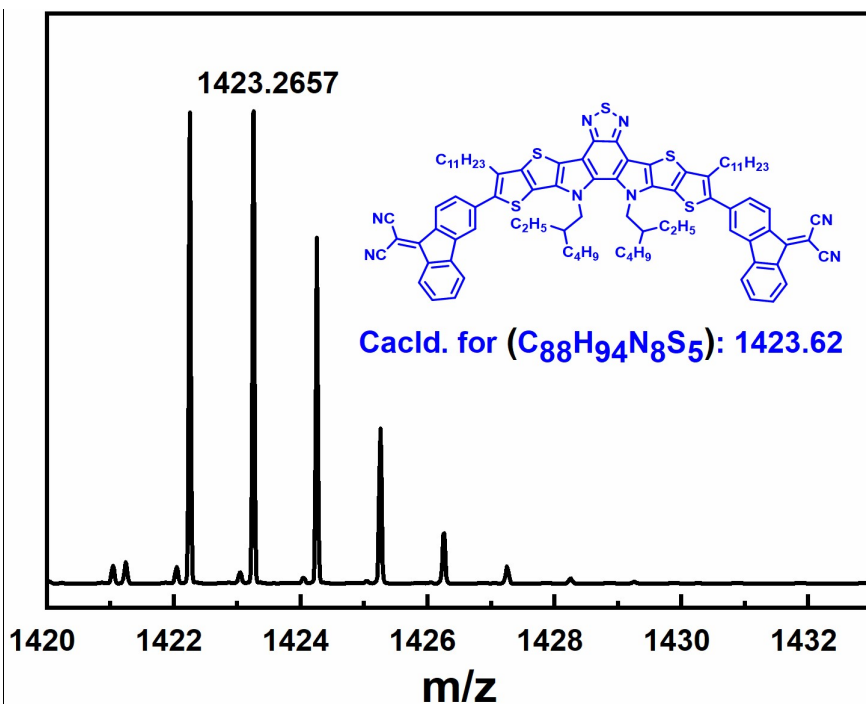


Fig. S5. The high resolution MALDI-TOF mass spectrum of YF-CN.

5 Additional Figures

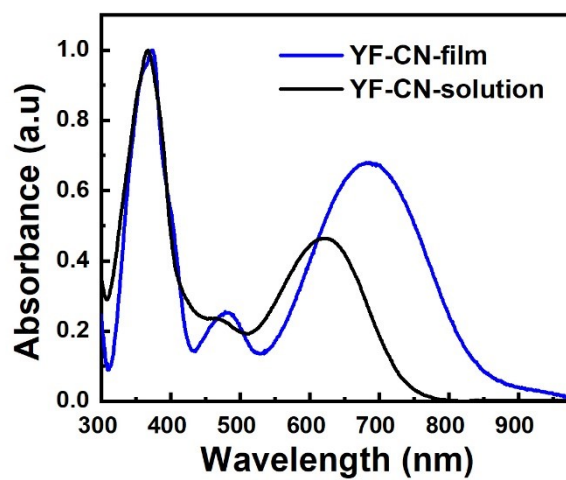


Fig. S6. Normalized absorption spectra of YF-CN in CHCl₃ solution and thin-film spin-coated with YF-CN in toluene solution.

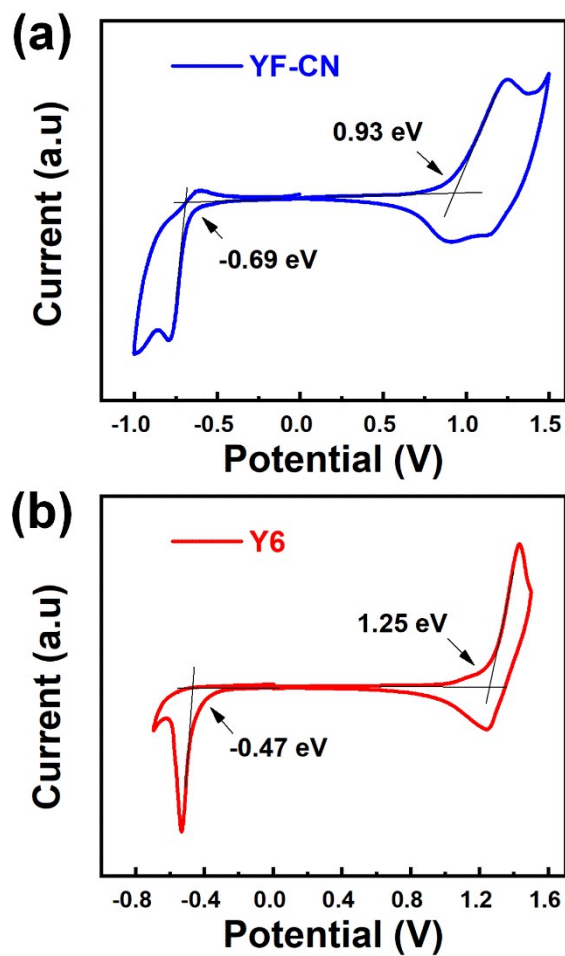


Fig. S7. Cyclic voltammetry of (a) YF-CN and (b) Y6.

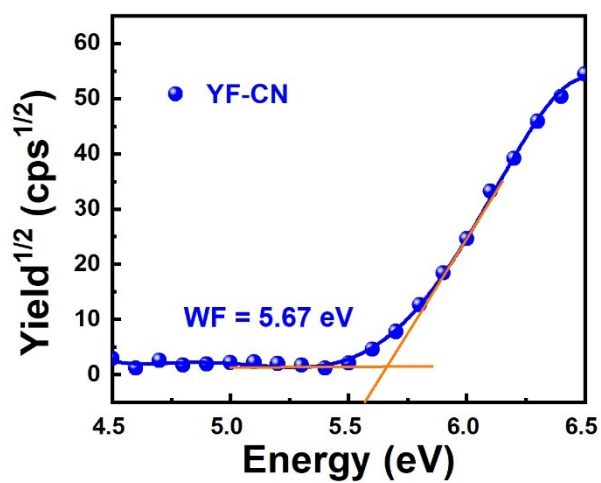


Fig. S8. UPS spectrum of the neat YF-CN film.

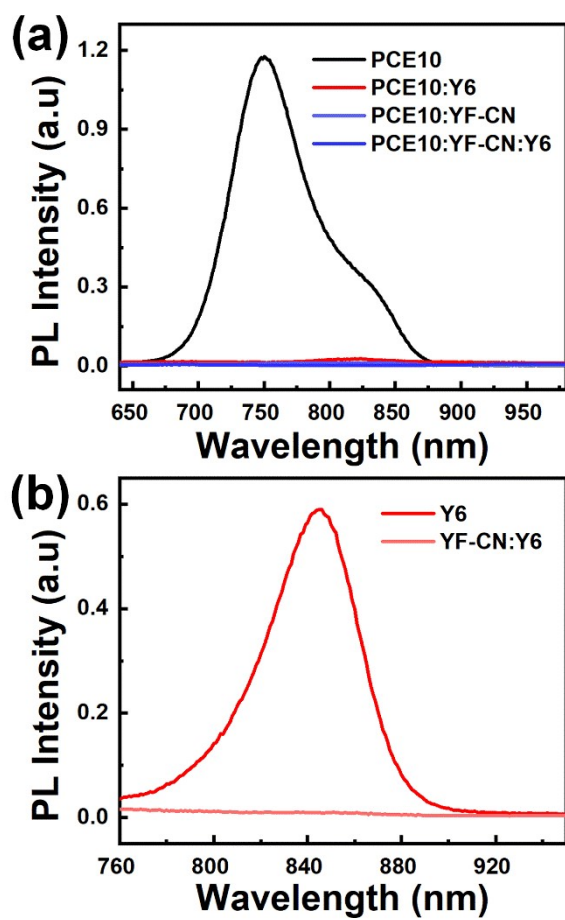


Fig. S9. Photoluminescence spectra of pure donor, acceptor and their blend films. (a) excited at 500 nm, (b) excited at 650 nm.

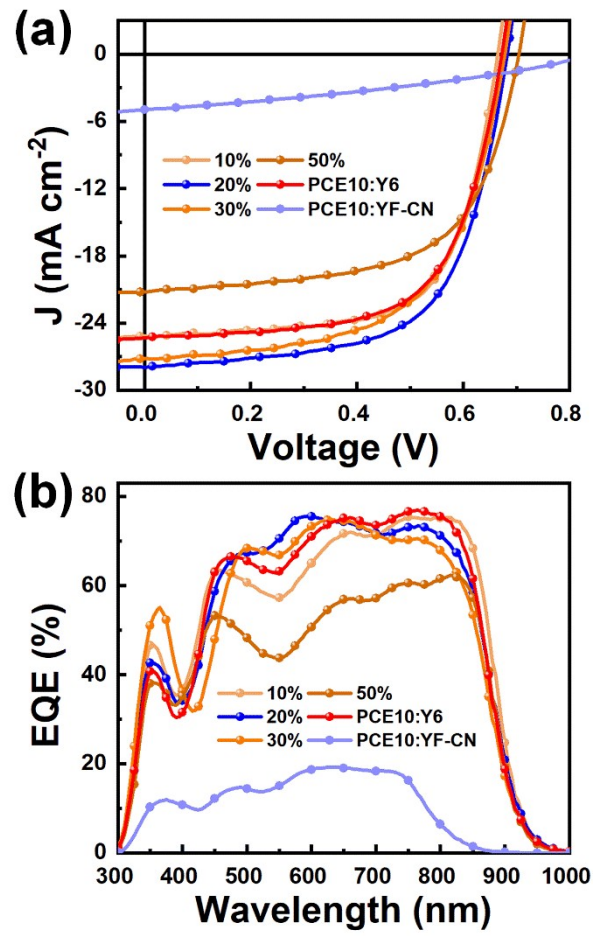


Fig. S10. (a) J-V curves and (b) EQE curves of PCE10:YF-CN:Y6-based ternary devices with different blending ratios.

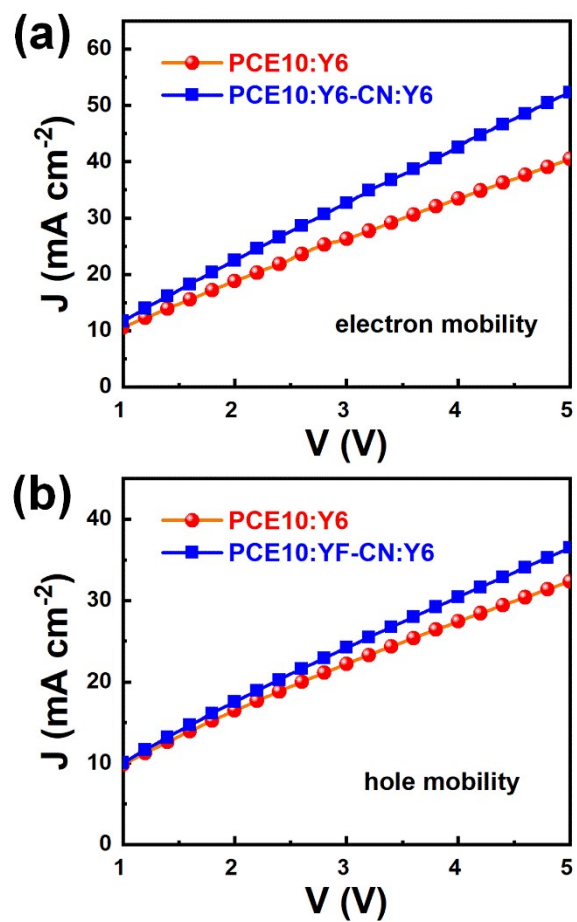


Fig. S11. Current density-voltage curves for the (a) electron and (b) hole mobility measurements of the blend films.

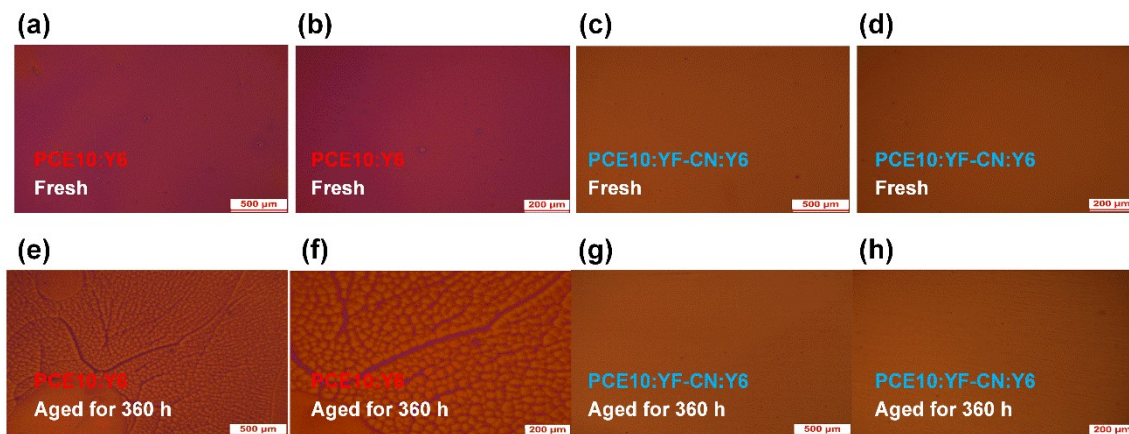


Fig. S12. Fluorescence microscopy images in different sizes for (a, b) fresh PCE10:Y6, (e, f) aged PCE10:Y6, (c, d) fresh PCE10:YF-CN:Y6 and (g, h) aged PCE10:YF-CN:Y6.

6 Additional Tables

Table S1. The photovoltaic parameters of the binary and ternary OSCs with different YF-CN ratio.

Active layer	Ratio	V_{oc} (V)	J_{sc} (mA cm ⁻²)	FF (%)	PCE (%)
PCE10:Y6	1:1.5	0.673	25.32	64.19	10.93
	0.9:0.1:1.5	0.664	25.14	66.78	11.16
PCE10:YF-CN:Y6	0.8:0.2:1.5	0.683	27.92	63.11	12.03
	0.7:0.3:1.5	0.678	27.15	60.21	11.08
	0.5:0.5:1.5	0.705	21.22	61.36	9.18
PCE10:YF-CN	1:1.5	0.839	4.97	33.78	1.41

Table S2. The electron mobilities (μ_e) and hole mobilities (μ_h) of the binary and ternary devices.

	$\mu_e/10^{-4}$ cm ² ·V ⁻¹ ·s ⁻¹	$\mu_h/10^{-4}$ cm ² ·V ⁻¹ ·s ⁻¹	μ_e/μ_h
PCE10:Y6	2.92	3.22	0.91
PCE10:YF-CN:Y6	5.71	3.55	1.61

Table S3. The photovoltaic parameters of the binary and ternary OSCs with the fresh and aged for 360 hours at room temperature.

Active layer	Store Conditions	V_{oc} (V)	J_{sc} (mA cm ⁻²)	FF (%)	PCE (%)
PCE10:Y6	Fresh	0.656	26.38	62.62	10.84
	Aged for 360 h	0.515	22.07	40.28	4.58
PCE10:YF-CN:Y6	Fresh	0.681	24.40	66.26	11.01
	Aged for 360 h	0.688	23.54	61.52	9.97

